Biochimie 95 (2013) 204–214

Contents lists available at SciVerse ScienceDirect

Biochimie

journal homepage: www.elsevier.com/locate/biochi

Research paper

Trifluoroethanol-induced conformational change of tetrameric and monomeric soybean agglutinin: Role of structural organization and implication for protein folding and stability

Anisur R. Molla, Dipak K. Mandal*

Department of Chemistry and Biochemistry, Presidency University, 86/1 College Street, West Bengal, Kolkata 700 073, India

ARTICLE INFO

Article history:
Received 18 April 2012
Accepted 13 September 2012
Available online 26 September 2012

Keywords:
Soybean agglutinin
β-Sheet lectin
Protein stability
Solvent perturbation

ABSTRACT

2,2,2-Trifuoroethanol (TFE)-induced conformational structure change of a β-sheet legume lectin, soybean agglutinin (SBA) has been investigated employing its exclusive structural forms in quaternary (tetramer) and tertiary (monomer) states, by far- and near-UV CD, FTIR, fluorescence, low temperature phosphorescence and chemical modification. Far-UV CD results show that, for SBA tetramer, native atypical β-conformation transforms to a highly α-helical structure, with the helical content reaching 57% in 95% TFE. For SBA monomer, atypical β-sheet first converts to typical β-sheet at low TFE concentration (10%), which then leads to a nonnative α-helix at higher TFE concentration. From temperature-dependent studies (5–60 °C) of TFE perturbation, typical β-sheet structure appears to be less stable than atypical β-sheet and the induced helix entails reduced thermal stability. The heat induced transitions are reversible except for atypical to typical β-sheet conversion. FTIR results reveal a partial α-helix conversion at high protein concentration but with quantitative yield. However, aggregation is detected with FTIR at lower TFE concentration, which disappears in more TFE. Near-UV CD, fluorescence and phosphorescence studies imply the existence of an intermediate with native-like secondary and tertiary structure, which could be related to the dissociation of tetramer to monomer. This has been further supported by concentration dependent far-UV CD studies. Chemical modification with N-bromosuccinimide (NBS) shows that all six tryptophans per monomer are solvent-exposed in the induced α-helical conformation. These results may provide novel and important insights into the perturbed folding problem of SBA in particular, and β-sheet oligomeric proteins in general.

1. Introduction

The problem of protein folding, in principle, envisions folding as a stochastic search of many conformations available to a polypeptide chain [1,2]. Thus, considerable experimental research has been directed towards detection of folding intermediates and their characterization including the factors governing their stability to gain insights into the interactions responsible for their formation as well as their role in protein folding [3–5]. Besides conformers having residual native-like secondary structures, there has been emphasis on the importance of nonnative secondary conformations in protein folding pathways. It has been hypothesized that all globular proteins, regardless of their native structure, fold via highly α-helical intermediate structures [6]. Recently, Chen et al. [7] has reported that formation of an α-helix can be a rate-limiting step during folding of a predominantly β-sheet protein. Nonnative states are easily obtained by solvent perturbation. An extensively studied cosolvent is 2,2,2-trifluoroethanol (TFE) which has been widely used to characterize secondary structure states in protein folding [8–10]. TFE tends to stabilize α-helical structures of proteins and peptides, and causes disruption of their native structures. Theoretical computational studies, using a two-dimensional lattice model, suggest that TFE mainly weakens nonlocal hydrophobic interactions and slightly favors local helical interactions [11]. Shiraki et al. [9] has proposed that helical propensity of the TFE-induced state is determined by local interaction based on the amino acid sequence. It has been shown that extensive helix formation in TFE does not occur when a protein has a very low intrinsic helix forming propensity [12]. However, the detailed mechanism of TFE action still remains unclear.

Abbreviations: SBA, soybean agglutinin, lectin from soybean (*Glycine max*); TFE, 2,2,2-trifluoroethanol; CD, circular dichroism; FTIR, Fourier transform infrared; NBS, N-bromosuccinimide.

* Corresponding author. Tel./fax: +91 33 2241 3893.
E-mail address: dm_pcchem@yahoo.co.in (D.K. Mandal).

0300-9084/$ – see front matter © 2012 Elsevier Masson SAS. All rights reserved.
http://dx.doi.org/10.1016/j.biochi.2012.09.011

Soybean agglutinin (SBA) is an oligomeric β-sheet protein, and belongs to the family of legume lectins. Lectins are carbohydrate-binding proteins that are involved in various biological recognition processes [13]. Further, many lectins are now important tools in biomedical research. The richest source of lectins is, however, the seeds of leguminous plants, and legume lectins are among the most extensively studied families of proteins. The members of this family show a high degree of homology in their tertiary structures, and display an oligomeric state as dimer or tetramer. SBA, which is specific for GalNAc/Gal, exists as a tetramer in the native state. Its three-dimensional structure has been determined by X-ray diffraction analysis [14,15]. The tertiary structure of SBA subunit is similar to that of other legume lectins such as concanavalin A [16], and describes a jelly roll motif that comprises three antiparallel β-sheets: a six-stranded flat 'back', a seven-stranded curved 'front', and a five-stranded 'top' that forms a roof-like structure above the other two (Fig. 1A). Two subunits of SBA dimerize by a side-by-side 'canonical' mode forming a continuous 12-stranded β-sheet. The tetrameric structure of the protein involves nearly parallel, back-to-back association of two such 'canonical' dimers that interact through contacts between their two outermost strands, creating a channel between them (Fig. 1B).

The TFE-induced secondary structure changes of this β-sheet lectin at the level of tetramer and monomer, and their implications in protein folding and stability would, therefore, constitute an interesting theme of study. A β-sheet to α-helix transition in presence of TFE for some legume lectins has been reported in the recent past [17–19]. For SBA, experimental studies on its unfolding and stability have been published in the last few years [20–22]. We have previously demonstrated that structured SBA monomer develops and accumulates during refolding from the completely unfolded state, and reconstitutes the tetramer with a kinetic mechanism involving monomer-to-dimer association as the rate-determining step [23]. Recently, we have shown that the tryptophan environment of SBA is characterized by unique structural and dynamic features that are maintained in specific quaternary and tertiary states [24]. In this article, we have explored the effects of TFE on the secondary structure perturbation of SBA tetramer and monomer by far-UV CD and FTIR. Further, tertiary/quaternary structure changes of TFE-induced states, using tryptophan as intrinsic probe, have been investigated by near-UV CD, fluorescence, low temperature phosphorescence and chemical modification. For the first time to our knowledge, this work presents TFE perturbation study on both the native oligomeric state, as well as its building block, namely, monomeric unit of a β-sheet lectin, which could provide new insight into this perturbed folding problem.

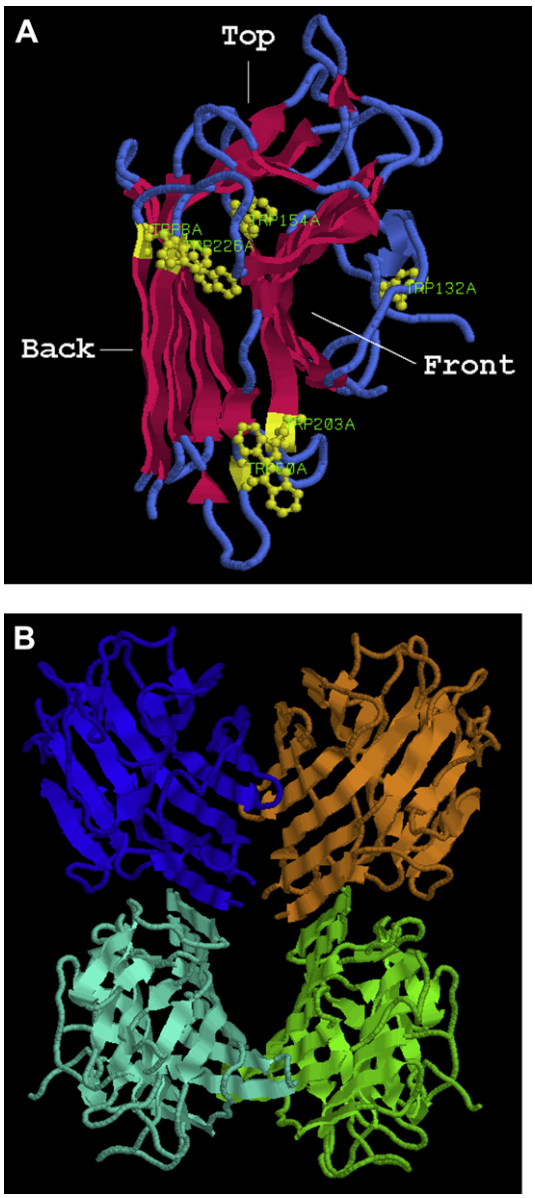

Fig. 1. (A) Structure of SBA monomer (PDB entry 2SBA) consisting of three β-sheets (a six-stranded 'back', a seven-stranded 'front' and a five-stranded 'top'). The six Trp residues are highlighted in yellow ball-and-stick. (B) Tetrameric structure of SBA, which involves nearly parallel back-to-back association of two 'canonical' dimers, each of which represents a continuous 12-stranded β-sheet formed by side-by-side alignment of six-stranded back β-sheets of two monomers. [For interpretation of color referred in this figure legend, the reader is referred to web version of the article.]

2. Materials and methods

2.1. Materials

Soybean flour, guar gum, deuterium oxide (D_2O) and 2,2,2-trifluoroethanol (TFE) were purchased from Sigma. Cross-linked guar gum matrix was prepared as described [25]. DCl was prepared by reaction of benzoyl chloride with D_2O and collected in D_2O. TFE-OD was obtained by distilling TFE with D_2O. All other reagents used were of analytical grade. All pH values reported in this paper denote apparent pH meter readings for solutions prepared in D_2O or in presence of TFE. Double distilled water was used throughout.

2.2. Protein purification

SBA was purified from the crude extract of soybean flour by affinity chromatography on cross-linked guar gum matrix [26]. As aggregation of SBA occurs on storage in the lyophilized state, affinity-purified SBA was precipitated by ammonium sulfate (80% saturation) and dialyzed against appropriate buffer before use in different experiments. However, for FTIR measurements, lyophilized SBA was used immediately. The integrity of quaternary structure of SBA was confirmed by size-exclusion chromatography on Sephadex G-100 in 10 mM sodium phosphate buffer, pH 7.2 when the protein was eluted as a single peak corresponding to its tetrameric molecular mass. The purity of the sample was also checked by sodium dodecyl sulfate-polyacrylamide gel electrophoresis (SDS-PAGE) [27]. Monomeric form of SBA was generated exclusively in 10 mM glycine–HCl buffer, pH 2.0 as described [24].

Protein concentration was determined spectrophotometrically using $A^{1\ \%,\ 1\ cm} = 12.8$ at 280 nm, and molar concentration was expressed in terms of monomer ($M_r = 30\ 000$) [28].

2.3. Steady-state absorption and fluorescence measurements

Ultraviolet absorption was measured in a Hitachi U 4100 double-beam spectrophotometer using Sigma cuvette (volume: 2 mL; path length: 1 cm).

Steady-state fluorescence measurements were done with a Hitachi F-7000 spectrofluorimeter (equipped with a 150 W xenon lamp) using Sigma cuvette (volume: 2 mL; path length: 1 cm). The excitation and emission band pass was 5 nm each, and scan speed was 60 nm/min. Samples without and in presence of TFE were prepared using tetrameric and monomeric SBA at pH 7.2 and 2.0, respectively, and allowed to reach equilibrium before fluorescence measurements were performed. All spectra were corrected by subtraction of corresponding blanks.

2.4. CD measurements

CD experiments were performed on a J-815 spectropolarimeter (Jasco, Japan) equipped with a Peltier type temperature controller. CD measurements in the far-UV and near-UV region were carried out using protein concentration of 10 μM (path length, 1 mm) and 50 μM (path length, 1 cm), respectively, except for the concentration dependent studies. Far-UV CD spectra were collected in the wavelength range of 260–190 nm, and near-UV in the region of 320–250 nm using scan speed of 50 nm/min and response time of 2 s. The spectra were averaged over at least five scans to eliminate signal noise. For performing temperature-dependent CD studies, SBA sample and TFE were pre-equilibrated at the desired temperature, and mixed thereafter. Measurements were made after the system reached equilibrium at the chosen temperature, and the spectra were corrected by subtraction of appropriate blanks. For thermal reversibility studies in the range of 20–60 °C, SBA samples in TFE were gradually raised to higher temperatures followed by a gradual decrease to lower temperatures. The data are represented as either ellipticity in mdeg or the mean residue ellipticity, $[\theta]$ which is defined as $[\theta] = 100\theta_{obs}/(lc)$, where θ_{obs} is the observed ellipticity in degrees, l is the length of the light path in centimeters, and c is the concentration in moles of residue per liter. All experiments with SBA tetramer were carried out in 10 mM phosphate buffer, pH 7.2 while those with SBA monomer were done in 10 mM glycine–HCl buffer, pH 2.0.

2.5. FTIR measurements

FTIR spectra were recorded on an FT/IR-680 plus spectrometer (Jasco, Japan) at room temperature at 4 cm^{-1} resolution as an average of 512 scans. For measuring FTIR spectra with tetrameric protein, native SBA was dissolved in D_2O containing 0.15 M NaCl, kept for 15 min and then placed in a sealed cell composed of two ZnSe windows and a Teflon spacer of 100 μm path length. Experiments in presence of TFE were performed in the same manner after adding required amounts of TFE-OD to SBA solution in D_2O containing 0.15 M NaCl, and the spectra were measured after 15 min. FTIR spectra of monomeric SBA were recorded in a similar fashion in absence or presence of TFE-OD except that the protein was dissolved in D_2O − 0.15 M NaCl solution adjusted to pH 2.0 with DCl. All measurements were carried out at protein concentration of 15 mg/mL, and appropriate blanks were subtracted in each case.

2.6. Phosphorescence measurements

Triplet state emissions were measured in a Hitachi F-7000 spectrofluorimeter equipped with phosphorescence accessories. Emission studies at 77 K were done using a Dewar system having a 5 mm o.d. quartz tube. All the samples of tetrameric and monomeric SBA without or in presence of TFE were made in 40% ethylene glycol in appropriate buffer. Freezing of the samples was done in liquid nitrogen immediately after mixing with ethylene glycol. The cryosolvent (40% ethylene glycol) used in the experiment was always found to form a clear glass. The samples were excited at 280 nm using a 10 nm band pass, and the emission band pass was 1.0 nm. The low temperature (77 K) spectra were found to be reproducible and free from any polarization artifacts.

2.7. Chemical modification

Oxidation of tryptophan to oxindolealanine with NBS [29] was performed at ambient temperature using different samples of SBA in absence and presence of TFE. TFE-perturbed states of SBA tetramer were oxidized in 20 mM sodium acetate buffer, pH 5.0 containing 0.15 M NaCl, and those of SBA monomer in 10 mM glycine–HCl buffer, pH 2.0 containing 0.15 M NaCl. Samples (500 μg/mL) were treated with aliquots of NBS (2 mM, freshly prepared) in a 1-cm path length cuvette. The reaction was followed by increase in absorbance at 250 nm (oxindolealanine) and decrease in absorbance at 280 nm (tryptophan). After 5 min incubation, the absorbance at 280 nm was recorded and corrected for dilution. The number of tryptophans oxidized by NBS was calculated as described by Spande and Witkop [29].

2.8. Reversibility of TFE solvation

SBA tetramer in 10 mM sodium phosphate buffer, pH 7.2 was mixed with TFE to a final concentration of 90% TFE. To test the reversibility of the process, the mixture was dialyzed extensively against the same buffer to remove TFE from sample. Similarly, TFE was removed from the mixture of monomeric SBA and 70% TFE by dialysis against 10 mM glycine–HCl buffer, pH 2.0. The samples obtained after removal of TFE were examined by far-UV CD and fluorescence.

3. Results and discussion

The conformational structure change of SBA as induced by the addition of TFE has been studied systematically with its two different and exclusive structural forms – tetramer and monomer, which are involved in the unfolding and refolding pathway of the protein [20–23]. The dimeric form of SBA, however, could not be isolated under any experimental conditions [23]. It has been proposed that TFE mimics the environment that occurs in proximity to biological membranes. Thus in vitro studies, as modeled by TFE additions, would reveal conformations that may be involved in protein folding, transport and degradation pathways in living cells or adopted under different stress and disease conditions [30,31].

3.1. Secondary structure characteristics of TFE-perturbed states of tetrameric and monomeric forms of SBA as observed by far-UV CD

Native SBA, as purified by affinity chromatography at pH 7.2, exists as a tetramer while the monomeric SBA has been generated in exclusive form at pH 2 [24]. Crystal structure of SBA shows that its secondary structure is predominantly β-sheet with no α-helix (Fig. 1) [14]. Fig. 2A shows the far-UV CD spectra of tetrameric SBA in increasing concentrations of TFE at 20 °C. Without TFE, native

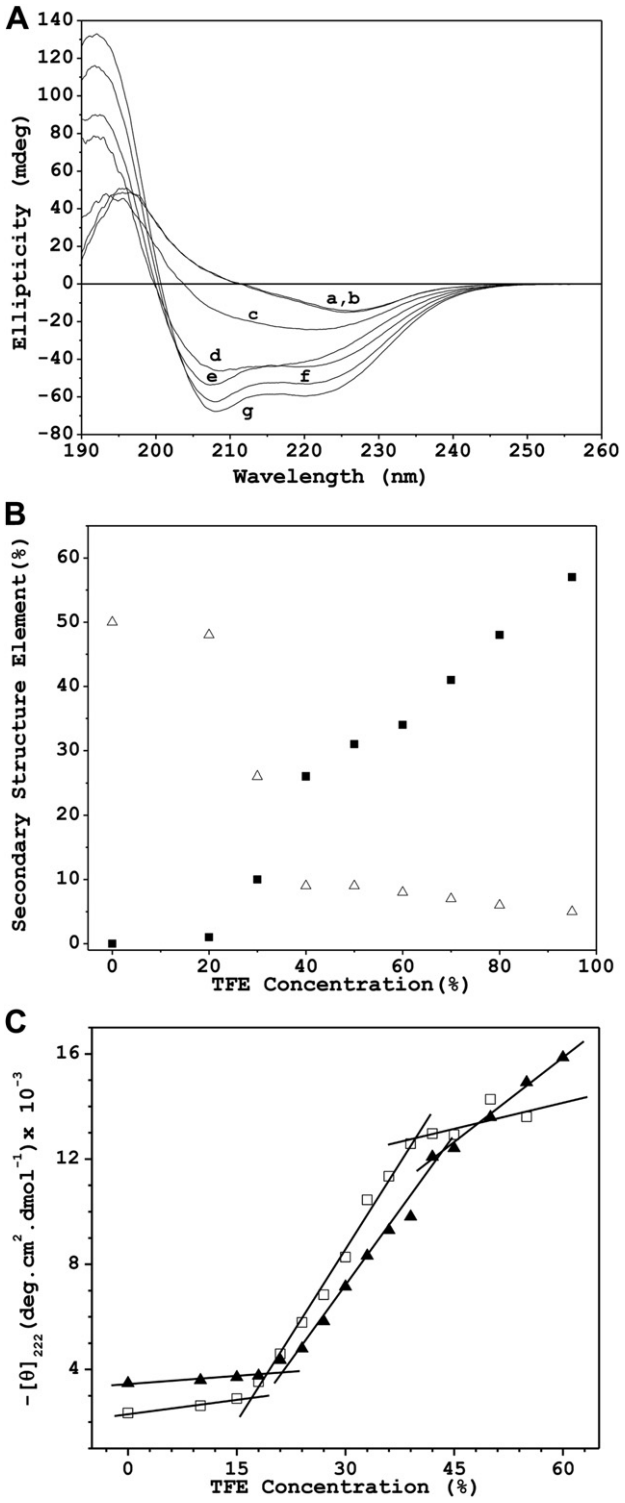

Fig. 2. (A) Far-UV CD spectra of SBA tetramer at pH 7.2 in presence of 0% (a), 20% (b), 30% (c), 40% (d), 60% (e), 80% (f) and 95% (g) TFE at 20 °C. Protein concentration was 0.32 mg/mL. Scan speed was fixed at 50 nm/min. Corresponding buffer spectra were subtracted in each case and at least five scans were performed. (B) Plot of β-sheet content (open triangle) and change of α-helix content (filled square) for SBA tetramer as a function of TFE concentration. Secondary structure components were estimated from analysis of far-UV CD spectra using CDNN software, version 2.1. See the text for details. (C) Plot of mean residue ellipticity at 222 nm, $[\theta]_{222}$, for SBA tetramer as a function of TFE concentration with 33 μg/mL (open square) and 600 μg/mL (filled triangle) of protein.

SBA exhibits an atypical β-sheet band shape having a characteristic negative peak at 226 nm along with a positive peak at 197 nm, which is consistent with the previous report [23]. This observation of atypical β-sheet as secondary structure element is well known for other legume lectins such as concanavalin A [17]. With addition of TFE, this atypical band shape remains constant up to 20% TFE. Thereafter, some broadening of the negative extremum occurs with increased TFE concentration and when TFE concentration is around 40%, the far-UV CD spectra begin to change and attain an α-helical structure characterized by two negative peaks at 220 nm and 208 nm. On further increase of TFE concentration up to a maximum of 95%, the spectra exhibit clearly the α-helical form with progressive rise of intensity, indicating more helical transformation. This is confirmed by estimation of protein secondary structure components from deconvolution of far-UV CD spectral data using CDNN software, version 2.1 [32]. The deconvolution results show ~50% β-sheet structure for native SBA tetramer comprising mainly the antiparallel component (44%), which is consistent with the crystallographic data. However, this analysis overestimates the helical component (~15%) when compared with crystal structure and FTIR analysis (shown below), which shows no or negligible α-helix. To depict the secondary structure changes associated with β-sheet to α-helix transformation in presence of TFE using far-UV CD, such overestimation of helical component is taken as a background data, based on which the progressive change in α-helix content is estimated. Fig. 2B shows a plot of change of secondary structure elements (β-sheet, α-helix) as a function of TFE concentration. As the TFE concentration is progressively increased, β-sheet content decreases and α-helical form increases gradually. At 40% TFE concentration, native β-sheet structure is largely lost and simultaneously a considerable amount of nonnative α-helical conformation (26%) is formed. With further increase in TFE concentration, the α-helical content continues to increase and becomes 57% in 95% TFE. It is seen from the deconvolution analysis that the random coil content decreases substantially (~20%) for change in TFE concentration from 40% to 95%. The more highly helical content in such high TFE concentration thus arises, at least in part, at the expense of random coil conformation. This might be possible as TFE raises the free energy of the random coil state, since TFE-water systems are less able to solvate the amide group of the peptide backbone. Consequently, TFE tends to favor states where the backbone amide groups form intramolecular hydrogen bonds, such as the α-helix [33].

The TFE-induced β-sheet to α-helix transition for SBA tetramer has been further examined using different protein concentrations in the range of 30–600 μg mL^{-1} Fig. 2C shows two transition profiles measured in terms of change of mean residue ellipticity at 222 nm, $[\theta]_{222}$, as a function of TFE concentration for SBA concentration of 33 and 600 μg mL^{-1}, respectively. The transition midpoint for the process is found at ~28% TFE for SBA concentration of 33 μg mL^{-1} and at ~32% TFE for 600 μg mL^{-1} SBA. The conformational transition thus shows a protein concentration dependence. In the concentration range of 30–600 μg mL^{-1}, the transition midpoint gradually shifts to the right indicating that this transition may involve subunit dissociation of SBA tetramer.

Fig. 3 shows the far-UV CD spectra of monomeric SBA in presence of various concentrations of TFE at pH 2. In absence of TFE, monomeric form of SBA exhibits almost identical atypical β-sheet band shape as for tetrameric SBA. However, in sharp contrast to SBA tetramer, the atypical CD band shape of monomeric SBA changes clearly to one typical of β-sheet having a negative peak at 215 nm on limited addition of TFE (10%). Increase of TFE concentration to the extent of 20% leads to enhancement of signal intensity of typical β-sheet structure. More addition of TFE then induces formation of α-helical conformation at ~30% TFE which is lower than that

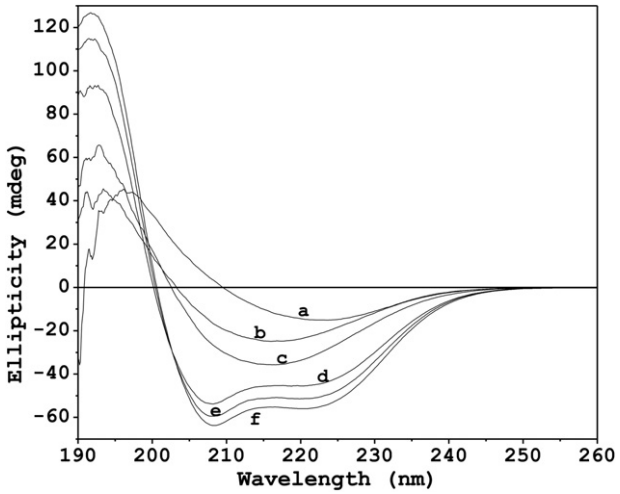

Fig. 3. Far-UV CD spectra of SBA monomer at pH 2 in presence of 0% (a), 10% (b), 20% (c), 30% (d), 50% (e) and 70% (f) TFE at 20 °C. Protein concentration was 0.3 mg/mL. Scan speed was fixed at 50 nm/min. Corresponding buffer spectra were subtracted in each case and at least five scans were performed.

required in case of SBA tetramer. Under this condition, the estimation by CDNN software indicates a total loss of β-sheet conformation. Further increase of TFE concentration leads to more helical conformation as evident from more intense α-helical band shape (Fig. 3). At a final concentration of 70% TFE, there occurs ~60% helical conformation which is similar to that obtained for SBA tetramer, though the TFE concentration needed in case of tetramer was much higher.

The effect of TFE in inducing secondary structure changes shows marked differences for the two structural forms of SBA. The structural organization of the protein thus appears to manifest its role for such perturbation effect. The native β-sheet structure for both SBA tetramer and generated monomer is atypical instead of typical β-sheet. In case of monomer, a relatively low concentration of TFE perturbs the atypical β-structure to a typical β-sheet conformation. It seems that TFE affects the nonlocal intramolecular hydrophobic interactions responsible for the structural restrictions for atypical conformation. In sharp contrast, for SBA tetramer, the atypical β-sheet is preserved even at higher TFE concentration (20%) and no clear TFE-induced atypical to typical β-sheet transition is discernible (Fig. 2A). It thus appears that oligomerization of the protein imparts greater stability to the secondary atypical β-sheet conformation in the SBA structure. As regards β-sheet to α-helix transformation, TFE exerts greater perturbing influence on the SBA monomer compared to the tetramer. Not only the growth of α-helical form but also the similar α-helical content has been obtained at lower TFE concentration for the monomer compared to the tetramer. This implies that the subunit association of SBA lends greater support for the integrity of secondary structural elements against solvent perturbation.

3.2. Effect of temperature on TFE-induced secondary structure changes for SBA tetramer and monomer

Perturbation of secondary structure of tetrameric and monomeric forms of SBA in presence of TFE was monitored by far-UV CD at various temperatures from 5 °C to 60 °C. Without TFE, the far-UV CD spectra of SBA tetramer remain practically invariant (not shown) within 5–60 °C. However, with TFE, such temperature variation exerts a significant influence on the secondary structure changes. Fig. 4A shows the far-UV CD spectra of native SBA at different TFE concentrations at 5 °C. As shown, the atypical β-sheet band shape is retained up to TFE concentration of at least 40%, and the spectrum shape changes to α-helical nature at 50% TFE or more. This indicates that lower temperature (less thermal energy) tends to inhibit initiation of secondary structure transformation so that helix induction requires higher TFE concentration. It is interesting to follow the far-UV CD spectra of tetrameric SBA in 20% TFE at different temperatures (5–60 °C) shown in Fig. 4B. In this case, the atypical β-sheet band shape remains unaltered up to 30 °C. With further rise of temperature the atypical band shape transforms predominantly to that of typical β-sheet up to 60 °C. These results suggest that typical β-sheet structure possesses more energy and hence thermally less stable than atypical β-sheet. Fig. 4C shows the far-UV CD spectra of native SBA in 95% TFE at various temperatures. As shown, α-helical band shape was obtained in the whole temperature range (5–60 °C), but loss of signal intensity was observed at temperature above 40 °C. It is estimated that there occurs ~20% less α-helix with concomitant increase of 'unordered' random coil structure within 40–60 °C. It appears that though helical transformation occurs at a low temperature in high TFE concentration, the α-helical structure is destabilized at higher temperature.

Unlike native SBA tetramer, the far-UV CD spectra of SBA monomer, in absence of TFE, do not show the same atypical β-sheet band shape within 5–60 °C (Fig. 5A). It starts losing its integrity around 40 °C. These results manifest that oligomerization of the protein tends to confer more stability of native secondary structure against heat perturbation. Fig. 5B shows the temperature dependent changes of secondary structure in 20% TFE. As is seen, the atypical β-sheet band shape transforms to typical shape (negative peak at ~216 nm) in the temperature range 5–30 °C, and helix induction ensues at higher temperature. In contrast, such atypical to typical transformation took place for SBA tetramer only at higher temperature around 50 °C (Fig. 4B). The far-UV CD spectra of SBA monomer exhibit α-helical form in ≥30% TFE at all temperatures (5–60 °C). However, the intensity of the α-helical signal decreases with rise in temperature as shown in Fig. 5C. These results agree with those for tetramer and further support that induced helix entails reduced thermal stability.

The reversibility of heat induced conformational transition for SBA tetramer and monomer has also been examined by far-UV CD. The results indicate reversible nature of heat induced transitions except the one involving atypical to typical β-sheet conversion. Fig. 4D shows a representative example for SBA tetramer in 60% TFE when the decreased intensity of induced α-helix at higher temperature is completely regained upon lowering the temperature. Further, the typical β-sheet to α-helical transition for SBA monomer upon heating is found to be reversible when the system is cooled to the same temperatures (data not shown). In contrast, atypical β-structure is not reformed from the typical one when the system is cooled (not shown). It appears that the nonlocal intramolecular hydrophobic interactions responsible for structural restrictions leading to atypical β-sheet are disrupted at higher temperature, which consequently yields typical β-secondary structure. Such disruption of nonlocal hydrophobic contacts of side chains turns out to be irreversible. The typical β-sheet conformation possesses more energy, and hence is less stable than atypical β-sheet structure. This might explain, in part, the driving force for the formation of atypical β-conformation in SBA and other legume lectins instead of typical β-sheet.

3.3. FTIR studies of TFE-induced conformational changes for SBA tetramer and monomer

FTIR spectroscopy provides valuable information about secondary structure content of proteins monitored primarily by

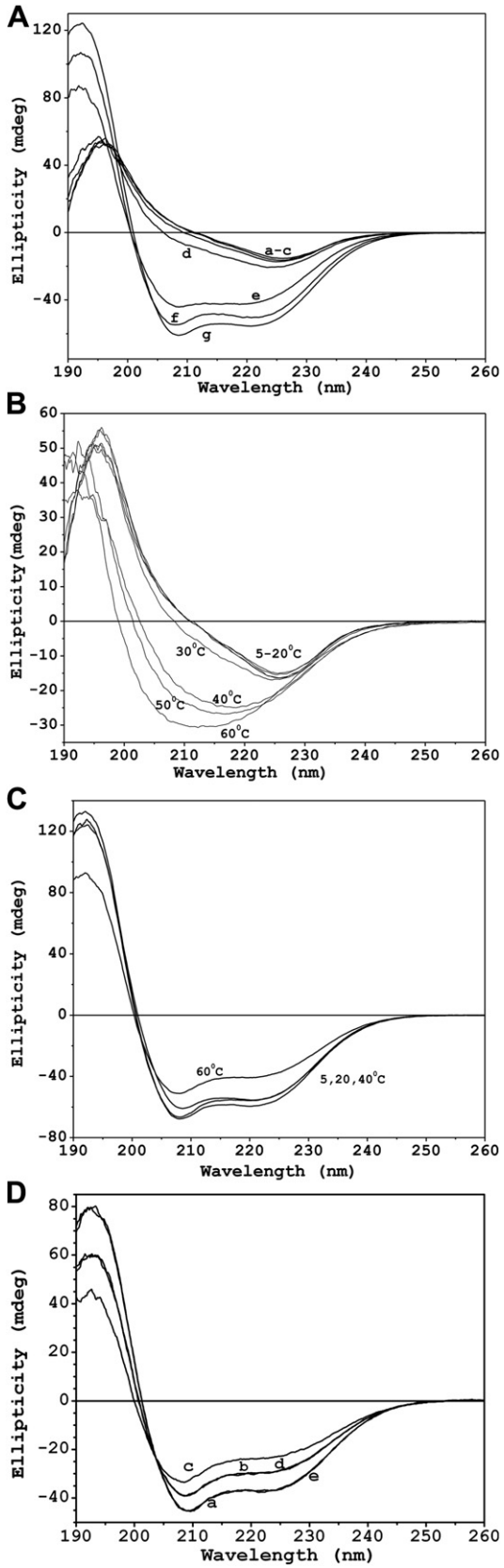

Fig. 4. Far-UV CD spectra of SBA tetramer at pH 7.2 in presence of (A) 0% (a), 20% (b), 30% (c), 40% (d), 50% (e), 70% (f) and 95% (g) TFE at 5 °C; (B) 20% TFE at different temperatures (5–60 °C) and (C) 95% TFE in the same temperature range (5–60 °C). SBA and TFE were equilibrated separately at a chosen temperature and mixed thereafter. Protein concentration was 0.32 mg/mL. (D) Far-UV CD spectra of SBA tetramer in presence of 60% TFE on heating progressively from 20 °C (a) to 40 °C (b) to 60 °C (c), and thereafter cooling back to 40 °C (d) and 20 °C (e). Protein concentration was 0.3 mg/mL. Corresponding buffer spectra were subtracted in each case and at least five scans were performed.

the characteristic amide I absorption band which is associated with mainly stretching vibrations of the C=O bond of the peptide linkage. This occurs because different elements of secondary structure (α-helix/β-sheet) have definite pattern of hydrogen bonding involving C=O groups [34,35]. Fig. 6A shows the FTIR spectra of SBA tetramer in absence and in presence of different concentrations of TFE-OD. Native SBA exhibits the amide I′ band (N-deuterated) at 1637 cm^{-1} characteristic of β-sheet structure. Analysis by protein secondary structure estimation software (JASCO, version 1.01.03) shows 53% β-sheet with negligible α-helix (Table 1). In presence of 90% TFE-OD (highest concentration achieved under experimental condition), an amide I′ peak is observed at 1652 cm^{-1} indicating transformation to α-helical conformation. Analysis of the spectra reveals that even under this high concentration of TFE-OD, the β-sheet to α-helix conversion is not complete (Table 1). However, the results clearly show that α-helix conformation results solely from the change of β-sheet as the yield of α-helix is almost same as the decrease in β-sheet content. Under somewhat lower TFE-OD concentration (80%), similar result of partial conversion to α-helical conformation takes place, though with smaller yield (Table 1). It may be mentioned that induced helical content obtained from FTIR analysis is lower than that obtained from far-UV CD deconvolution. Such variances are due to the difference in sample conditions used in the two techniques, viz., much higher protein concentration (15 mg/mL) used in FTIR compared to a low protein concentration (0.3 mg/mL) necessary for far-UV CD measurements.

The FTIR spectra of SBA monomer in absence and in presence of different concentrations of TFE-OD are shown in Fig. 6B. An amide I′ band is observed for SBA monomer at 1638 cm^{-1} indicating a dominant β-sheet structure similar to SBA tetramer. Analysis of the spectrum gives a β-sheet content of 54% with no α-helix (Table 1). In 80% TFE-OD, a prominent amide I′ peak is obtained at 1652 cm^{-1} along with the band at 1638 cm^{-1}, which indicates conversion to a partial α-helical conformation. Under this condition, it is estimated that 32% of α-helix has been induced through transformation of about the same amount of β-sheet (Table 1). The results are in overall agreement with those obtained from far-UV CD studies except that the extent of conversion monitored by FTIR is less due to the difference in experimental conditions in the two methods.

FTIR measurements have also been performed with lower TFE concentrations (20–50%). Under these conditions, both forms of SBA show visible precipitation. It is evident from the FTIR spectra (Fig. 6A and B) that there occurs, besides the characteristic bands for β-sheet and α-helix, a peak at ~1618 cm^{-1} along with a shoulder at ~1683 cm^{-1}, which is characteristic of aggregation [36]. It is interesting to note that protein concentration is observed to be another factor for the conformation and stability of the TFE-induced states of both SBA tetramer and monomer. No aggregation was found during CD measurement done at low protein concentrations. In contrast, aggregation/precipitation was observed in FTIR studies under high protein concentrations in 20–50% TFE. The low-frequency band at ~1618 cm^{-1} is indicative of the spectral characteristics of intermolecular β-sheet structure and has no spectral equivalent for monomeric intramolecular sheet formation [37]. It seems that high protein concentration would tend to accelerate aggregation as may be expected for a conformational

change based on protein–protein interactions. However, under high TFE concentrations (80–90%), the aggregation peak is observed to disappear. It therefore appears that high TFE concentration shifts the balance from intermolecular β-sheet formation to intramolecular helical segment formation. This might be possible because high TFE concentration leads to significant loss of tertiary structure, thereby breaking up presumed hydrophobically driven interactions for aggregate formation. In contrast, under relatively low TFE environment, while the amount of exposed hydrophobic surface area increases presumably after formation of helical intermediate along with significant retention of tertiary structure, an energetically competitive possibility might arise for intermolecular β-structure formation being further assisted by higher protein concentration. Such a process may find relevance to amyloid-forming proteins and peptides which often aggregate via helix to sheet transformation [38,39].

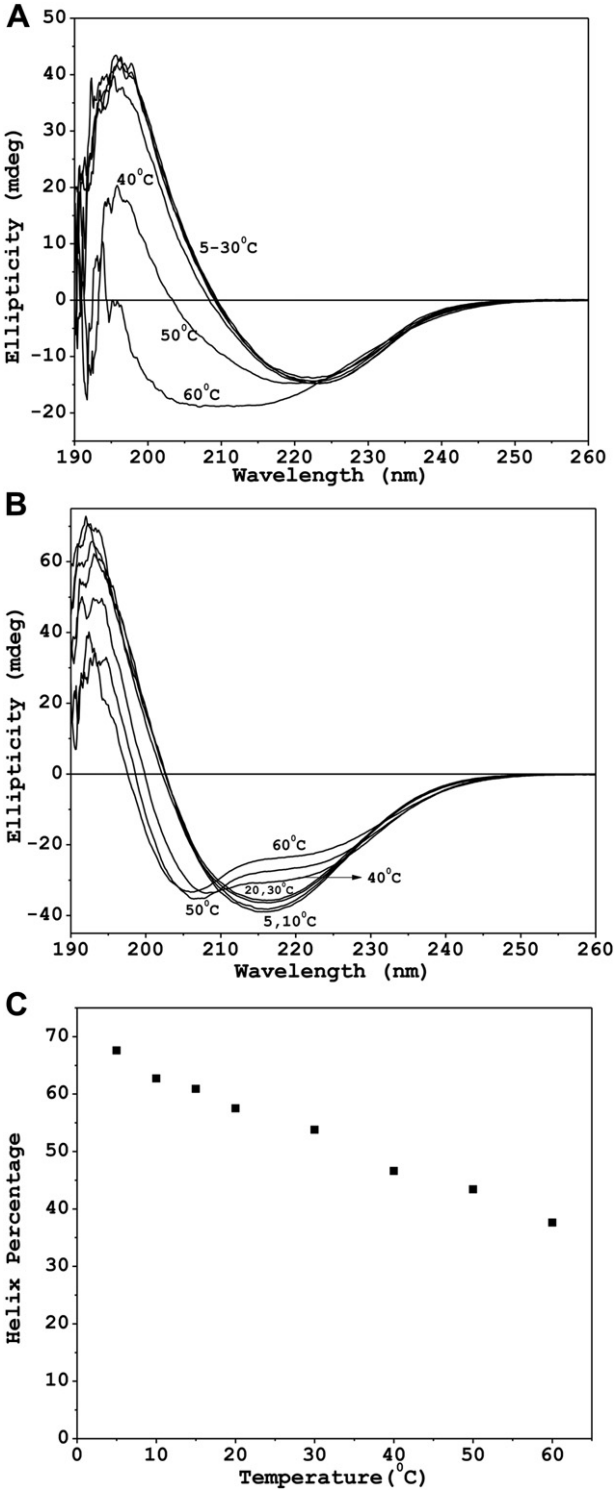

Fig. 5. Far-UV CD spectra of SBA monomer at different temperatures (5–60 °C) (A) without TFE and (B) in presence of 20% TFE. SBA and TFE were equilibrated separately at a particular temperature and mixed thereafter. Protein concentration was 0.3 mg/mL. Appropriate blanks were subtracted in each case and average of at least five scans was taken. (C) Plot of α-helix content for SBA monomer in presence of 70% TFE as a function of temperature. Amount of secondary structure components were estimated from analysis of far-UV CD spectra using CDNN software, version 2.1.

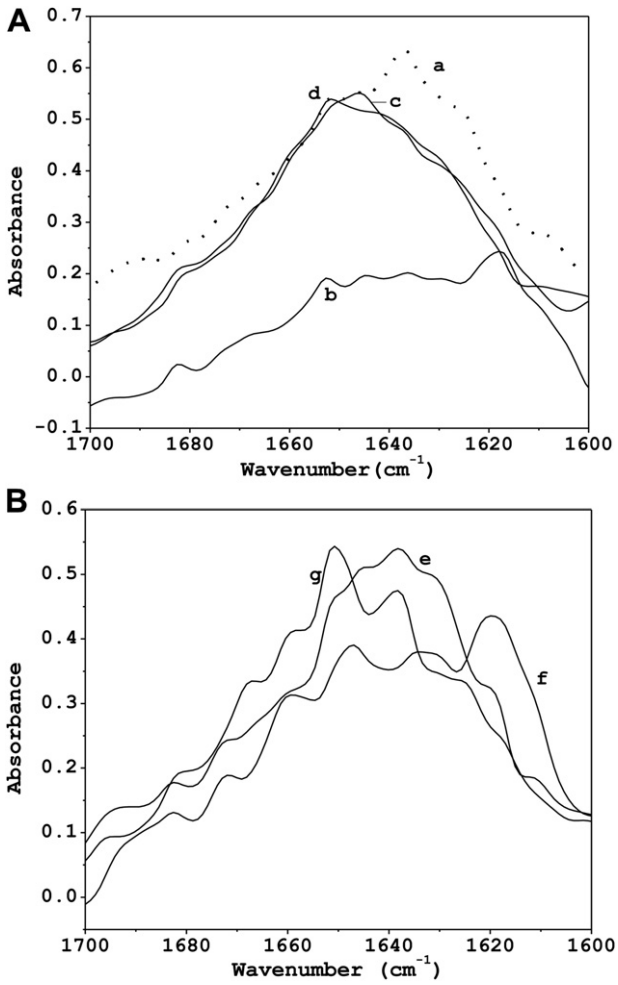

Fig. 6. FTIR amide I′ spectra of (A) SBA tetramer in presence of 0% (a), 35% (b), 80% (c) and 90% (d) TFE-OD; and (B) SBA monomer with 0% (e), 50% (f) and 80% TFE-OD (g). Protein concentration was 15 mg/mL. Spectra were recorded at 4 cm^{-1} resolution as an average of 512 scans. Corresponding buffer spectra were subtracted in each case.

Table 1
Estimation of β-sheet and α-helix from analysis of FTIR spectra of SBA tetramer and monomer in absence and presence of TFE.

System	β-Sheet	α-Helix
Tetramer	53	3
Tetramer + 80% TFE-OD	32	24
Tetramer + 90% TFE-OD	26	31
Monomer	54	0
Monomer + 80% TFE-OD	25	32

3.4. Near-UV CD and fluorescence studies

Near-UV CD and fluorescence techniques sample tertiary structure of proteins and provide important information on the environment and packing arrangement of aromatic amino acid residues [40,41]. The change in tertiary structure as monitored by near-UV CD for tetrameric SBA in absence and presence of various concentrations of TFE at 20 °C is shown in Fig. 7A. For native SBA tetramer, positive maxima at 287 and 280 nm are observed. These spectral shapes indicate almost compact tertiary structure of SBA tetramer at pH 7.2. As shown, the tertiary structure is preserved up to 20% TFE, and at TFE concentration ≥ 40%, the tertiary structure of SBA tetramer gets completely lost. These results, when compared with secondary structure changes monitored by far-UV CD, indicate that TFE-induced change in tertiary structure is concomitant with alteration of secondary structure from β-sheet to α-helix. Fig. 7B shows near-UV CD spectra of SBA monomer in the absence and with various concentrations of TFE. In the absence of TFE, the spectrum exhibits similar shape with broad band at 287 and 280 nm as for the tetramer; however, an additional band around 273 nm is observed which seems to originate from solvent exposure of Tyr residues following dissociation of tetramer to monomer. Interestingly, addition of 10% TFE to SBA monomer causes loss of tertiary structure. These results are in contrast to those for SBA tetramer in the sense that collapse of tertiary structure of SBA monomer starts earlier with atypical to typical β-sheet change which ultimately leads to α-helical transition.

Fig. 8 shows the plot of fluorescence maxima for SBA tetramer and monomer as a function of TFE concentration at ambient temperature. Emission maxima of both tetramer (328 ± 1 nm) and monomer (336±1 nm) are red shifted with increase in TFE concentration and finally reach to 346 ± 1 nm. These results indicate increased solvent exposure of tryptophan residues by disruption of quaternary/tertiary structure, and are in overall agreement with the results obtained from near-UV CD studies. However, it is interesting to note the change in fluorescence maximum for SBA tetramer from 328 nm to 337 nm in 20–30% TFE. The red shift of emission maximum clearly signifies increased solvent exposure of tryptophan residues possibly due to quaternary dissociation [24]. This result agrees well with that obtained from concentration dependent studies by far-UV CD.

3.5. Phosphorescence studies at low temperature (77 K)

Phosphorescence studies of proteins at low temperature (in a suitable cryosolvent) provide structured spectra with a characteristic (0,0) band, which reveal the immediate environment of the tryptophan residues [42]. The phosphorescence spectra at 77 K of SBA tetramer and monomer in presence of different concentrations of TFE are shown in Fig. 9A and B, respectively. As shown in Fig. 9A, the two (0,0) bands at 409.2 and 414.2 nm, in consistent with our earlier work [24] coalesce to a single band which is gradually blue shifted with increasing TFE concentration and finally reaches to 408.2 nm in 90% TFE. It is also seen that at ~30% TFE, the (0,0) band occurs at 411.4 nm which resembles the band for monomeric SBA [24]. Thus, under such TFE environment, SBA tetramer may dissociate to monomer species with mostly intact secondary and tertiary structure, which are in excellent agreement of the results obtained from far-UV CD and fluorescence studies described above. The blue-shifted phosphorescence can be attributed to the lower polarizability of the environment and the less stabilization of the triplet state by rigid solvation geometry for the exposed tryptophans.

For SBA monomer, the position of (0,0) band shows similar trend with addition of TFE and shifts from 412 nm (in absence of TFE) to 407.8 nm in 70% TFE (Fig. 9B). At higher TFE concentrations, collapse of tertiary structure takes place concomitantly with

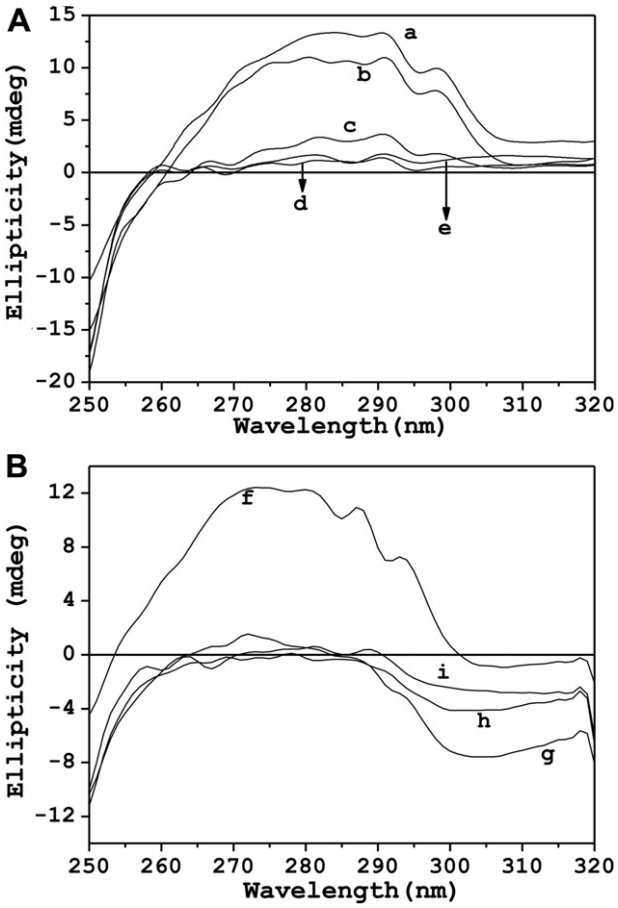

Fig. 7. Near-UV CD spectra at 20 °C of (A) SBA tetramer with 0% (a), 20% (b), 40% (c), 50% (d) and 60% (e) TFE; and (B) SBA monomer with 0% (f), 10% (g), 30% (h) and 50% (i) TFE. Protein concentration was 1.5 mg/mL. Scan speed was fixed at 50 nm/min. Corresponding buffer spectra were subtracted in each case and at least five scans were performed.

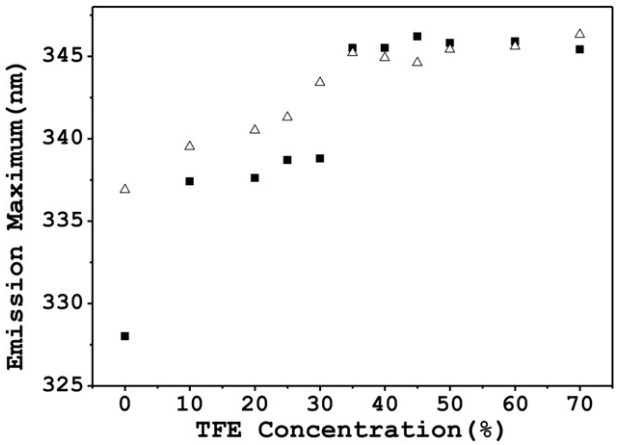

Fig. 8. Plot of fluorescence emission maximum of SBA tetramer (filled square) and monomer (open triangle) as a function of TFE concentration at ambient temperature. Protein concentration was 0.1 mg/mL. Excitation wavelength was 280 nm. Scan speed was fixed at 60 nm/min. Corresponding blanks were subtracted in each case.

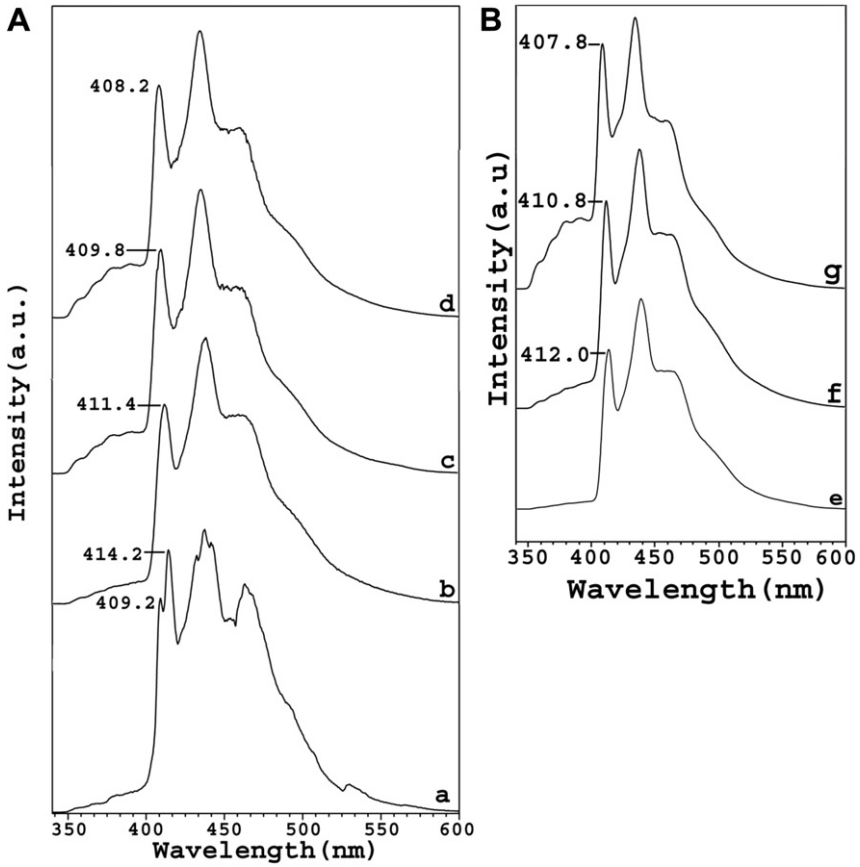

Fig. 9. Phosphorescence spectra of (A) SBA tetramer in 0% (a), 30% (b), 70% (c) and 90% (d) TFE; and (B) SBA monomer in 0% (e), 30% (f), 70% (g). Protein concentration was 20 μM in each case. Excitation wavelength, 280 nm; excitation and emission band passes were 10 and 1.0 nm, respectively.

changes of secondary structure for both forms of SBA tetramer and monomer. When the final TFE-induced state is attained with a major α-helical conformation, the fluorescence signal is red shifted to 346 nm and the phosphorescence (0,0) band appears around 408 nm. These results are reminiscent of the tryptophan environment of the denatured form obtained in the denaturant-induced unfolding of the protein [24].

3.6. Chemical modification studies

Tryptophans in proteins can be modified selectively with N-bromosuccinimide (NBS), thus allowing to probe their environment in protein structure. The reaction is rapid converting the indole side chain to oxindole, and leads to a loss of tryptophan fluorescence and a decrease in absorbance at 280 nm. However, NBS reaction of TFE-perturbed states of tetrameric SBA could not be done below TFE concentration of 50% as precipitation occurred under the experimental condition. Estimation of tryptophan modification shows that five tryptophan residues per monomer could be oxidized in presence of 70–90% TFE. However, fluorescence spectra of the NBS-oxidized samples show a weak peak at 305 nm and no characteristic tryptophan emission maximum, thus indicating absence of any tryptophan residue. A little lower estimate of five instead of six tryptophan residues may arise from error in absorption data due to possible occurrence of aggregation during the period of measurement. The oxidation results for TFE-perturbed state of SBA monomer in 50% TFE, however, show that all six tryptophans are modified. These results thus provide further evidence that TFE induces a helical structure for both tetramer and monomer in which all the tryptophan residues become exposed to the solvent.

3.7. Reversibility of TFE-induced states

The TFE-induced transition of native β-sheet to nonnative α-helix conformation for both SBA tetramer and monomer was examined with respect to a plausible reversible process. After the generation of α-helical form, TFE was removed by extensive dialysis, and the resulting protein samples were characterized by CD and fluorescence. The far-UV CD spectra of these samples for SBA tetramer and monomer are shown in Fig. 10A and B, respectively. It is seen that the α-helical band disappears, and band shapes characteristic of typical (instead of atypical) β-sheet at ~215 nm are obtained in cases of both tetrameric and monomeric forms. When examined by fluorescence, the emission maximum is found to shift from 346 nm (α-helical states) to 337 nm which is characteristic of tertiary monomeric structure (spectra not shown).

It turns out that the β-sheet to α-helical transformation for SBA tetramer and monomer with TFE is not completely reversible. An irreversible step appears to involve the β-sheet structure when its native atypical conformation transforms to a nonnative typical one. It is interesting to note that reversibility studies of heat induced conformational transition as described before also indicate reversible nature of transitions except the one involving atypical to typical β-sheet conversion. It seems that the nonlocal intramolecular hydrophobic interactions responsible for atypical structure in the native state are not restored on removal of the denaturing influence of TFE/heat.

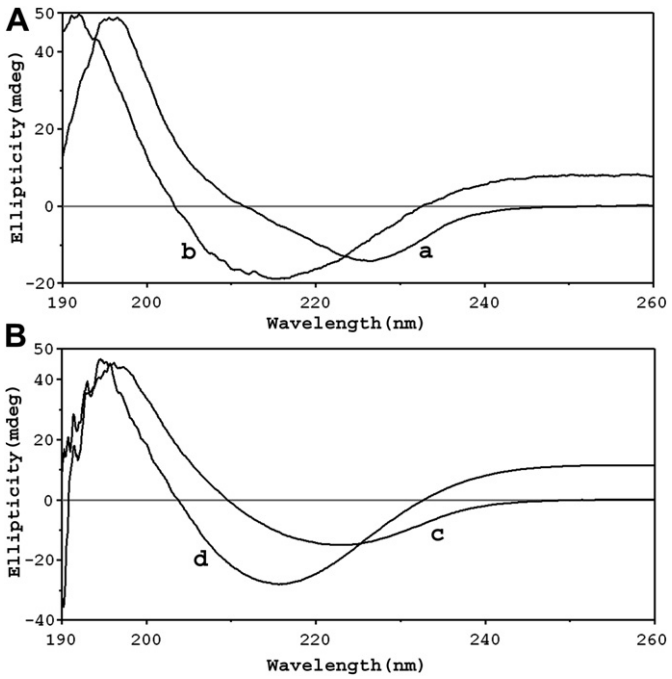

Fig. 10. (A) Normalized Far-UV CD spectra at pH 7.2 of SBA tetramer without TFE (a) and SBA sample after TFE removal from the mixture of SBA tetramer and 90% TFE (b). (B) Normalized far-UV CD spectra at pH 2 of SBA monomer without TFE (c) and SBA sample after TFE removal from the mixture of SBA monomer and 70% TFE (d). Scan speed was fixed at 50 nm/min. Blanks were subtracted and at least five scans were performed in each case.

4. Conclusions

To our knowledge, this work appears to be the first systematic study of TFE-induced perturbation utilizing both oligomeric and monomeric units of an oligomeric lectin. The TFE perturbation process for tetrameric form of SBA, **T(β)**, could be delineated in terms of the following scheme:

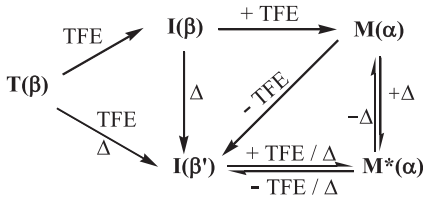

where **I(β)** is a relatively stable intermediate with mostly intact native atypical β-secondary conformation and monomeric tertiary structure, **M(α)** is the final TFE-induced state having a major nonnative α-helical conformation with loss of native tertiary structure, **I(β′)** is an intermediate with nonnative typical β-secondary conformation, and **M*(α)** is the TFE-induced state analogous to **M(α)** but differing in terms of α-helix content. The process for the monomeric form of SBA, **M(β)**, could be represented as

$$\mathbf{M}(\beta) \longrightarrow \mathbf{I}(\beta') \overset{+\mathrm{TFE}}{\underset{-\mathrm{TFE}}{\rightleftharpoons}} \mathbf{M}(\alpha)$$

where **I(β′)** is an intermediate structure with nonnative typical β-secondary conformation, and **M(α)** is the final TFE-induced state having a major nonnative α-helical conformation but no stable tertiary structure.

The present study provides novel insights on the subtle role of structural organization (tertiary *vs* quaternary association) of SBA in the TFE-induced changes of native β-structure to nonnative conformations, and the energetic preference for native secondary β-structure being atypical rather than a typical one. It has been suggested that TFE-induced helicity is indicative of α-helical propensity based on the amino acid sequence [43]. TFE is thus not a helix-inducing solvent in the sense that it will induce helix formation independently of the sequence but rather a helix-enhancing cosolvent, which promotes helices for regions with some helical propensity [44]. Peptides with profound helical propensity often reach the maximum helical content at relatively lower TFE concentration (30–50%) while maximum stabilizing effect of TFE is reached at much higher concentration (80%) with peptides whose inherent propensities are small [44]. Presumably, the formation of α-helical form of SBA under TFE solvation may arise from the helical propensity of the amino acid sequence, which might suggest a possibility of non-hierarchical model of protein folding involving the formation of native β-sheet being preceded by α-helix as has been proposed for β-lactoglobulin [9].

Acknowledgements

This work was supported by research grant (No. 02/(0028)/11/EMR-II) from the Council of Scientific and Industrial Research (CSIR), Government of India. We thank the anonymous reviewers for helpful suggestions.

References

[1] K.A. Dill, H.S. Chan, From Levinthal to pathways to funnels, Nat. Struct. Biol. 4 (1997) 10–19.
[2] M.M. Garcia-Mira, M. Sadqi, N. Fischer, J.M. Sanchez-Ruiz, V. Munoz, Experimental identification of downhill protein folding, Science 298 (2002) 2191–2195.
[3] O.B. Ptitsyn, Kinetic and equilibrium intermediates in protein folding, Protein Eng. 7 (1994) 593–596.
[4] R. Jaenicke, H. Lilie, Folding and association of oligomeric and multimeric proteins, Adv. Protein Chem. 53 (2000) 329–397.
[5] D. Sen, D.K. Mandal, Pea lectin unfolding reveals a unique molten globule fragment chain, Biochimie 93 (2011) 409–417.
[6] V.I. Lim, Polypeptide chain folding through a highly helical intermediate as a general principle of globular protein structure formation, FEBS Lett. 89 (1978) 10–14.
[7] E. Chen, M.L. Everett, Z.E. Holzknecht, R.A. Holzknecht, S.S. Lin, D.E. Bowles, W. Parker, Short-lived α-helical intermediates in the folding of β-sheet proteins, Biochemistry 49 (2010) 5609–5619.
[8] M. Buck, S.E. Radford, C.M. Dobson, A partially folded state of hen egg white lysozyme in trifluoroethanol: structural characterization and implication for protein folding, Biochemistry 32 (1993) 669–678.
[9] K. Shiraki, K. Nishikawa, Y. Goto, Trifluoroethanol-induced stabilization of the alpha-helical structure of beta-lactoglobulin: implication for non-hierarchical protein folding, J. Mol. Biol. 245 (1995) 180–194.
[10] Y. Luo, R.L. Baldwin, Trifluoroethanol stabilize the pH4 folding intermediate of sperm whale apomyoglobin, J. Mol. Biol. 279 (1998) 49–57.
[11] P.D. Thomas, K.A. Dill, Local and nonlocal interactions in globular proteins and mechanisms of alcohol denaturation, Protein Sci. 2 (1993) 2050–2065.
[12] N. Schönbrunner, J. Wey, J. Engels, H. Georg, T. Kiefhaber, Native-like β-structure in a trifluoroethanol-induced partially folded state of the all-β-sheet protein tendamistat, J. Mol. Biol. 260 (1996) 432–445.
[13] H. Lis, N. Sharon, Lectins: carbohydrate-specific proteins that mediate cellular recognition, Chem. Rev. 98 (1998) 637–674.
[14] A. Dessen, D. Gupta, S. Sabesan, C.F. Brewer, J.C. Sacchettini, X-ray crystal structure of the soybean agglutinin cross-linked with a biantennary analog of the blood group I carbohydrate antigen, Biochemistry 34 (1995) 4933–4942.
[15] L.R. Olsen, A. Dessen, D. Gupta, S. Sabesan, J.C. Sacchettini, C.F. Brewer, X-ray crystallographic studies of unique cross-linked lattices between four isomeric biantennary oligosaccharides and soybean agglutinin, Biochemistry 36 (1997) 15073–15080.
[16] A. Deacon, T. Gleichmann, A.J. Kalb, H. Price, J. Raftery, G. Bradbrook, J. Yariv, J.R. Helliwell, The structure of concanavalin A and its bound solvent determined with small- molecule accuracy at 0.94 Å resolution, J. Chem. Soc. Faraday Trans. 93 (1997) 4305–4312.
[17] Q. Xu, T.A. Keiderling, Trifluoroethanol-induced unfolding of concanavalin A: equilibrium and time-resolved optical spectroscopic studies, Biochemistry 44 (2005) 7976–7987.

[18] F. Naseem, R.H. Khan, Characterization of a common intermediate of pea lectin in the folding pathway induced by TFE and HFIP, Biochim. Biophys. Acta 1723 (2005) 192–200.
[19] S. Dev, R.H. Khan, A. Surolia, 2,2,2-Trifluoroethanol-induced structural change of peanut agglutinin at different pH: a comparative account, IUBMB Life 58 (2006) 473–479.
[20] M. Ghosh, D.K. Mandal, Analysis of equilibrium dissociation and unfolding in denaturants of soybean agglutinin and two of its derivatives, Int. J. Biol. Macromol. 29 (2001) 273–280.
[21] N. Keith, A.J. Parodi, J.J. Caramelo, Glycoprotein tertiary and quaternary structures are monitored by the same quality control mechanism, J. Biol. Chem. 280 (2005) 18138–18141.
[22] S. Sinha, A. Surolia, Oligomerization endows enormous stability to soybean agglutinin: a comparison of the stability of monomer and tetramer of soybean agglutinin, Biophys. J. 88 (2005) 4243–4251.
[23] M. Chatterjee, D.K. Mandal, Kinetic analysis of subunit oligomerization of the legume lectin soybean agglutinin, Biochemistry 42 (2003) 12217–12222.
[24] A.R. Molla, S.S. Maity, S. Ghosh, D.K. Mandal, Organization and dynamics of tryptophan residues in tetrameric and monomeric soybean agglutinin: studies by steady-state and time-resolved fluorescence, phosphorescence and chemical modification, Biochimie 91 (2009) 857–867.
[25] S. Ghosh, D.K. Mandal, Kinetic stability plays a dominant role in the denaturant-induced unfolding of *Erythrina indica* lectin, Biochim. Biophys. Acta 1764 (2006) 1021–1028.
[26] D.K. Mandal, C.F. Brewer, Interactions of concanavalin A with glycoproteins: formation of homogeneous glycoprotein-lectin cross-linked complexes in mixed precipitation systems, Biochemistry 31 (1992) 12602–12609.
[27] U.K. Laemmli, Cleavage of structural proteins during the assembly of the head of bacteriophage T4, Nature 227 (1970) 680–685.
[28] R. Lotan, H.W. Siegelman, H. Lis, N. Sharon, Subunit structure of soybean agglutinin, J. Biol. Chem. 246 (1974) 1219–1224.
[29] T.F. Spande, B. Witkop, Determination of the tryptophan content of proteins with N-bromosuccinimide, Methods Enzymol. 11 (1967) 498–506.
[30] L.A. Munishkina, C. Phelan, V.N. Uversky, A.L. Fink, Conformational behavior and aggregation of α-synuclein in organic solvents: modeling the effects of membranes, Biochemistry 42 (2003) 2720–2730.
[31] M. Perham, J. Liao, P. Wittung-Stafshede, Different effects of alcohols on conformational switchovers in α-helical and β-sheet protein models, Biochemistry 45 (2006) 7740–7749.
[32] G. Böhm, CDNN: CD Spectra Deconvolution Software Version 2.1, University of Halle- Wittenberg, Halle, 1997.
[33] J.K. Myers, C.N. Pace, J.M. Scholtz, Trifluoroethanol effects on helix propensity and electrostatic interactions in the helical peptide from ribonuclease T_1, Protein Sci. 7 (1998) 383–388.
[34] A. Barth, Infrared spectroscopy of proteins, Biochim. Biophys. Acta 1767 (2007) 1073–1101.
[35] M. Jackson, H.H. Mantsch, The use and misuse of FTIR spectroscopy in the determination of protein structure, Crit. Rev. Biochem. Mol. Biol. 30 (1995) 95–120.
[36] A.A. Ismail, H.H. Mantsch, P.T. Wong, Aggregation of chymotrypsinogen: portrait by infrared spectroscopy, Biochim. Biophys. Acta 1121 (1992) 183–188.
[37] J. Kubelka, T.A. Keiderling, Differentiation of beta-sheet-forming structures: ab initio-based simulations of IR absorption and vibrational CD for model peptide and protein beta- sheets, J. Am. Chem. Soc. 123 (2001) 12048–12058.
[38] S. Srisailam, T.K. Kumar, D. Rajalingam, K.M. Kathir, H.S. Sheu, F.J. Jan, P. Chao, C. Yu, Amyloid-like fibril formation in an all -barrel protein. Partially structured intermediate state(s) is a precursor for fibril formation, J. Biol. Chem. 278 (2003) 17701–17709.
[39] I. Pallares, J. Vendrell, F.X. Aviles, S. Ventura, Amyloid fibril formation by partially structured intermediate state of alpha-chymotrypsin, J. Mol. Biol. 342 (2004) 321–331.
[40] S.M. Kelly, T.J. Jess, N.C. Price, How to study proteins by circular dichroism, Biochim. Biophys. Acta 1751 (2005) 119–139.
[41] P. Mandal, D.K. Mandal, Localization and environment of tryptophans in different structural states of concanavalin A, J. Fluoresc. 21 (2011) 2123–2132.
[42] S. Ghosh, A. Misra, A. Ozarowski, C. Stuart, A.H. Maki, Characterization of the tryptophan residues of *Escherichia coli* alkaline phosphatase by phosphorescence and optically detected magnetic resonance spectroscopy, Biochemistry 40 (2001) 15024–15030.
[43] S.R. Lehrman, J.L. Tuls, M. Lund, Peptide alpha-helicity in aqueous trifluoroethanol: correlations with predicted alpha-helicity and the secondary structure of the corresponding regions of bovine growth hormone, Biochemistry 29 (1990) 5590–5596.
[44] F.D. Sonnichsen, J.E. Van Eyk, R.S. Hodges, B.D. Sykes, Effect of trifluoroethanol on protein secondary structure: an NMR and CD study using a synthetic actin peptide, Biochemistry 31 (1992) 8790–8798.